Set of instrumentation and methodological instructions for practical work in optics

Victor V. Dyomin

Tomsk State University, 634050 Tomsk, Russia

Igor G. Polovtsev

Design and Technological Institute "Optika", Siberian Branch of the
Russian Academy of Sciences, 634055 Tomsk, Russia

ABSTRACT

The opportunity to perform demonstrations and laboratory works in optics based on united compact equipment set is shown. Basic technique approaches and design are considered. The list of demonstrations and laboratory works is suggested. The techniques and their instrumental facilitation can be easily rearranged both for high and for secondary schools.

Keywords: optics, training equipment, compact installation, methodological instructions, optical experiments, Denisyuk hologram, double-exposed hologram

1. INTRODUCTION

Teaching demonstration and laboratory works in optics are usually perfomed on models made for definite demonstration only or on scientific equipment which is quite sophisticated for educational process. It leads to overloading of educational laboratory by cumbersome, highly specified and expensive equipment. In addition, techniques for different subjects differ a lot. Device description and instructions occupy the main part of operating manuals. The above factors make the accepting of educational programs and extending of more successful tecniques difficult.

Methodical approaches and designs allowing to simplify and unify training equipment in optics are considered which gives an opportunity to concentrate an attention on phenomenon researched instead of on instrumental provision. In addition, training technique exchange becomes rathereasy.

These problems have been solved the following aspects.

The equipment has to be a modular construction with blocks which are easily replaced.

It is necessary to use a laser as a radiation source. Modified optical schemes should be applied for demonstrations of some classical experiments.

In correspondence with principles mentioned above we have developed a compact (it can be easy placed on a usual table), portable (its weight is less than 10 kg), easily used equipment. Its use as a modular construction gives an opportunity to apply a small quantity of optical elements which are easily replaced and at the same time provides carring out of all classical experiments in optics. This equipment can be specified for educational process both of high and secondary schools by changing of element set. Simplicity and unification of holders give a chance to add the set of optical elements.

High coherence of laser radiation permits not to use precision mechanical units and narrow-band filters. High power density of laser beam enables one to apply a low-power laser (~ 2 mw). This laser and aluminium screen (200x200 mm) with a mat surface are enough for majority of diffraction and interference effects demonstrations in shadowed room for 15-20 people. And they are more than enough for individual laboratory work.

Operating models of this equipment developed and produced by specialists from the Tomsk State University, Design and Technological Institute "Optika" of Siberian Branch of the Russian Academy of Sciences, and Optikon Ltd. These models are used now in a number of institutes and schools of Siberian region.

This training equipment provides performing of demonstrations and laboratory works and recording of Denisyuk holograms as well.

2. CONSTRUCTION OF THE INSTRUMENT

The construction of the instrument is schematically shown in Fig. 1.

This set consist of a frame (22) attached by optical bench (23). A He-Ne laser (1) with power supply (25), turning units (26,27) with adjusting screws (28,29) are placed in the frame (22). Turning mirrors (2,3) are fixed on the turning units. Microlens (5) is fixed in the frame (22) by means of screw (30), microlens (5-1) is used in collimator (6).

An adjusted table (31) for holography is placed in a recess of the frame (22). This table can be fixed at a required height by means of screws (32) located on both sides of the frame . An ajusting frame (34) is fixed on horizontal surface of the frame by screws (33). Either photographic plate for hologram recording or a metal plate (36) with turning mirror (4) are fastened inside of the adjusting frame by fixing arms (35). The adjustment of the mirror (4) is realized by screw (37).

The optical bench (23) is connected to the frame (22) either horizontally (fig. 1) or vertically (fig. 1a) by an adapter (42). The adapter (42) is fixed on the frame (22) instead of an adjusting frame (34). Ground glass or measurement screens (20,21) are installed within a required distance by means of supports.

A collimator (6), the difraction gratings (7-1 - 7-7), lenses (8-1, 8, 9), one (10-1), two (10-2) or three (10-3) pin holes, half-plane (11), microlens (5) in an additional rim (43) can be installed on the optical bench (23) with help of pillars (38).

A spherical mirror is included in the set. It can be used in experiments as optical element as well as the lenses (8, 8-1, 9). All optical elements have unified mountings which permit them to be fixed easily in holders (38).

The Lloyd mirror (17) is situated on a separate pillar. Its adjustment is realized by screw (39).

The pillar (44) is designed for Hartle device (45) mounting on the optical bench (23). Turning holder (46) and inserting support (47) can be placed in this pillar too.

Individual table (48) is designed for installation of optical elements out of optical bench (23). Carriers (38), inserting support (47), cylinder cell (49), photodiode (50) (with holder (51) and carrier (38)) can be fixed on this table.

Inserting support (47) is used for suitable setting of plane-parallel cell (52) but it is possible to apply it for placement of other objects into laser beam.

3. WAVE OPTICS EXPERIMENTS

3.1. Diffraction experiments

With a laser, the classical diffraction experiments, for instance the diffraction on a single hole, two holes, on a half-plane, on a slit, do not demand any special forming of light beam and they are realized by placing of diffraction elements required (10-1, 10-2, 10-3, 11, 12) (fig. 1) into non-expanded laser beam.

The scale made on the screen (21) permits to measure slit and hole dimensions from difraction pattern using well-known formulae .

In addition to the above experiments ., observation of diffraction pattern from holes system (for instance, three holes) is interesting and informative. Removing the screen (20) from diffraction element (10-3), it is easy to explain a notion of a far zone of diffraction and demonstrate invariance of diffraction pattern in this zone relative to transverse shift of the diffraction element. We can illustrate the same effect using licopodium particles monolayer on the glass base as a system of screens.

It is advisible to discuss the experiments with diffraction gratings in a separate chapter. The training eguipment includes the following diffraction gratings : linear grating with a 10 μm period (7-1) and the one with a 20 μm period (7-2); linear double gratings with 10 μm (7-3) and 20 μm (7-4) periods, respectively; linear triple grating with 50 μm period; circular gratings (7-6, 7-7).The gratings were made of optical glass therefore they are not sensitive to working conditions and they can be used for a long time. Holographic diffraction elements can be included into this set as well. Besides of exciting demonstrations it is easy to measure a grating constant and radiation wavelength.

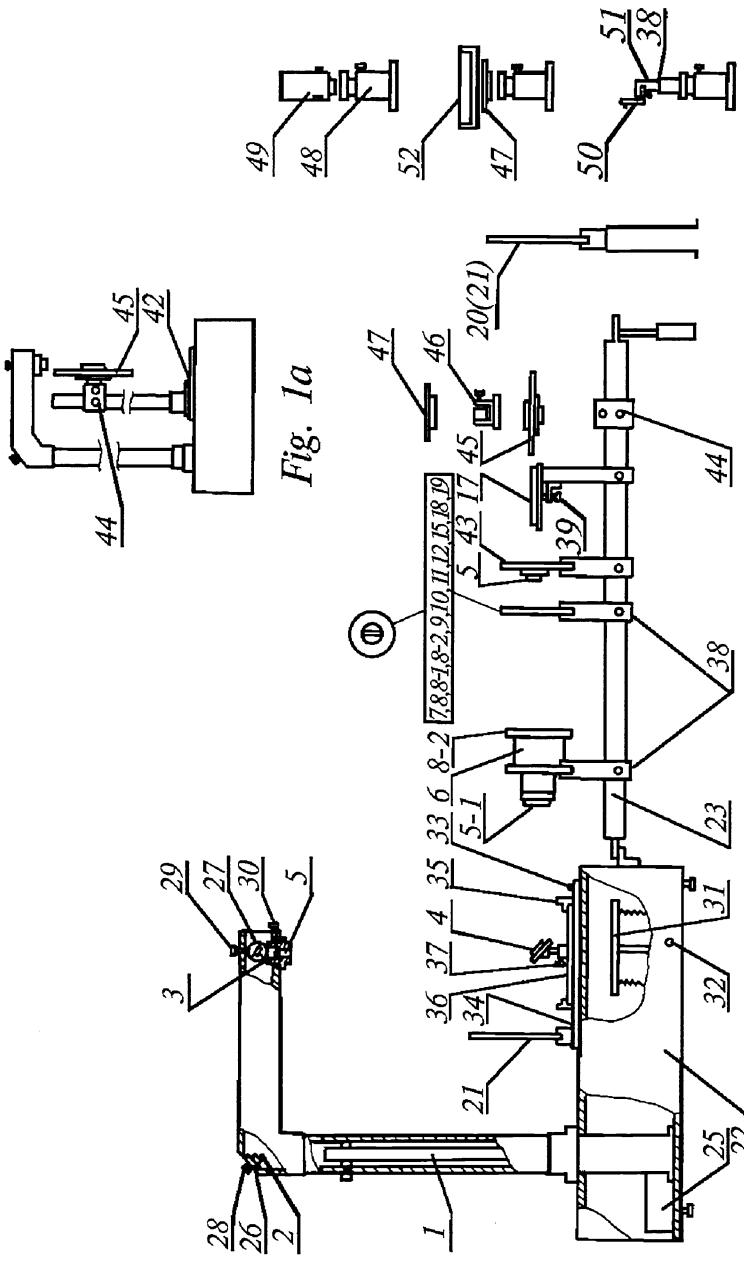
49
48
52
47
51
38
50
20(21)
47
46
45
44
45
42
44
7,8,8-1,8-2,9,10,11,12,15,18,19
43
17
39
5
38
8-2
6
5-1
33
23
35
31
4
37
32
36
34
21
25
22
29
27
30
5
3
28
26
2
1

Fig. 1a

Fig. 1

Diffraction patterns from crossed and circular gratings can be a model imaging of X-ray diffraction on crystals and polycrystals, respectively. Note that diffraction on circular grating is demonstrated on scheme in fig. 2.

The same scheme allows us to measure a focal length of lense (8). For this purpose it is suitable to use a linear grating with a known period d (grating period d can be measured preliminary using a diffraction pattern).

The screen (21) is placed in focal plane of lens (8). Clear focusing of all diffraction orders observed on the screen is a guideline of this. The focal length f is derived from the formulae:

$$2d \sin\Theta = \lambda,$$

$$\mathrm{tg}\Theta = \frac{r}{f},$$

where λ is radiation wavelength; Θ is diffraction angle, r is distance between central and the first diffraction order on the screen (21).

Using two (or system) holes instead of grating it is simple to explain a Hartmann method and show identity of the pattern in far zone of diffraction and the pattern in a lens focal plane.

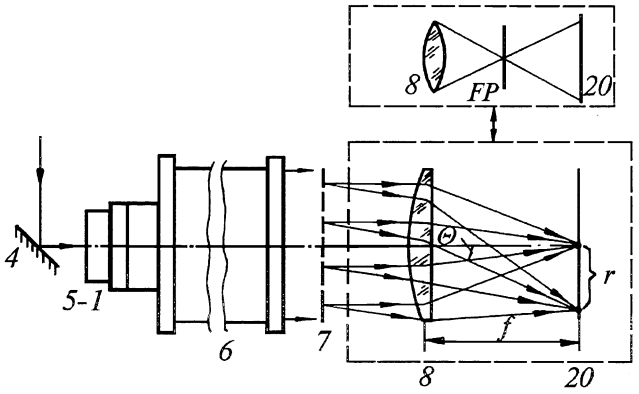

Fig. 2. Sheme for determination a lens' focal length. 4 - turning mirror; 5-1 - microlens ; 6 - collimator; 7 - diffraction grating; 8 - converging lens ; 20 - screen; FP - Fourier plane (Fourier optics demonstrations)

Application of monodisperse medium volume as a diffraction object makes posiblle to model a small angles method widely used in disperse media optics.

3.2. Polarization experiments

This set uses He-Ne laser with elliptical polarization of radiation. Two polarization filters should be used in experiments as a polarizer and an analizer. Alternatively, we can demonstrate an elliptical light polarization and only one polarizer is necessary in this case.

We can study Malus law by applying of two filters. The demonstration of polarization change phenomenon by means of placing depolarizing object between the polarizer and the analyzer is also possible.

Note that nonexpanded beam is usable in the above experiments due to small power of the used laser. This condition is obligatory for Malus law studying only because of a small sguare of the applied photodetector. But expanded (by lens (9), fig. 1) or collimated (by collimator (6), fig. 2) beam is much proper for observation of maximum radiation attenuation between the crossed polarizer and analyzer.

3.3. Interference experiments

Well-known interference experiments, as a rule, are carried out with point sources because this is the simplest method to get radiation coherence. This condition is not obligatory when a high coherence laser is used. But it is efficient to give an explanation on equivalent schemes which show point sources arrangement. This permits to clearly explain the concepts of space and temporal coherence and make a base for interpretation of more complicated interference patterns in the wave optics and holography.

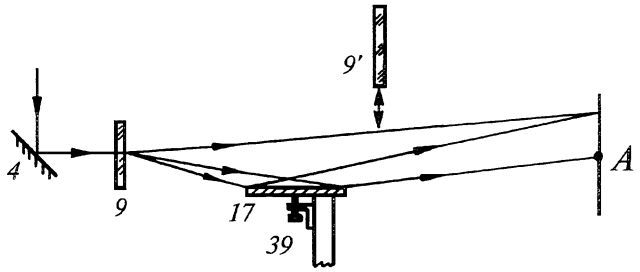

Fig. 3. Scheme for interference pattern demonstration with the Lloyd mirror. 4 - turning mirror; 9 (9') - diverging lens; 17 - mirror; 39 - ajusting screw; 20 - screen.

The scheme for observation of interference pattern with Lloyd mirror is presented on fig.3. The second lens (9') can be applied for picture magnification. A diffraction pattern from mirror (17) edge is superimposed on the interference pattern near the point A on the screen (20).

In contrast to the interference pattern the first one doesn't change under mirror (17) inclination by screw (39). The interference fringes are observed on the screen (20). The boundaries of dark and light fringes are broken lines which show mirror surface defects. In general, the equivalent scheme of two arbitrary arranged point sources is true for this demonstration. However, in practice we usually realize a grazing beam incidence on the Lloyd mirror to get reasonable interference fringes. It corresponds to disposition of two point sources in one wave front.

The same equivalent scheme is realized for Young experiment demonstration when a pair of "point" holes is placed into nonexpanded laser beam. The observed pattern is interesting for analysis because it is "an interference of two diffraction patterns". Strictly speaking, the diffraction pattern from a real-size hole is an envelope of interference pattern from two point sources. It is easy to measure a distance between the holes using well-known formulae.

The scheme suggested for Newton rings demonstration is shown in fig. 4. A diverging lens (9) is used here twice: first, it is applied to get a divergent beam (4-9-8) and then (8-9-20) to magnify the dimensions of interference pattern made by waves reflected from spherical and plane lens (8) surfaces. This scheme can be realized only with small angles between (4-9-8) and (8-9-20) directions. So we can consider it equivalent to the coaxial disposition of point sources.

Using this scheme (fig. 4) we can measure a radius of curvature R of lens (8) spherical surface. First, a diaphragm with the known dimension x_1 should be placed close to lens (8) and a dimension of illuminated screen(20) part x_2 must be measured.

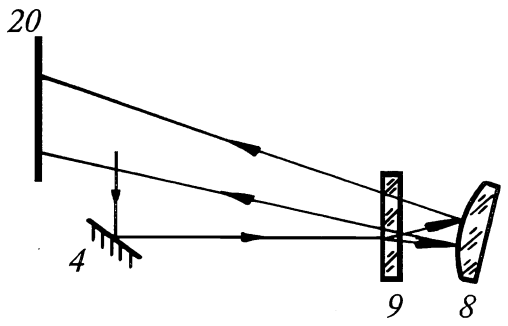

Fig. 4. Scheme for Newton rings demonstration.
4 - turning mirror; 9 - diverging lens; 8 - plano-convex lens; 20 - screen.

We define a lens magnification on path (8-9-20) as: $\delta = x_2 / x_1$. Then we define r_i and r_{i-j} by use of the scale made on the screen. Here r_i is a radius of interference ring number i and r_{i-j} is a radius of interference ring number i-j. The formula for radius R is the following:

$$R = [(r_i/\delta)^2 - (r_{i-j}/\delta)^2]/\lambda_j$$

The Gauss formula for the plano-convex lens is simple: $f = r/(n-1)$, where n=1,52 is a refractive index of lens material. Therefore it is easy to definite the lens focal length in this experiment and then to compare it with the one obtained according to chapter 3 technigue.

It should be noted that the pattern observed in this experiment is not classical Newton rings. Actually, in classical Newton experiment phase difference appears in the air gap between a convex lens surface and a plane that the lens occupies. However, it brings to the only difference between patterns resulted from Newton experiment and the above pattern. The dark spot (minimum) is always occured in the middle of the classical Newton pattern. In our case, this spot can be both dark and bright in accordance with lens thickness in the midlle and beam incidence

We suggest to use a wedge with small (near 30") angle to observe an interference of beams propagating at an angle to each other. The interference pattern is occured in a large distance range from wedge to screen for both divergent and parallel beams. Curved fringes which are like Newton rings are seen in the first case, and equidistant

straight fringes are observed in the second one. Removing (or bringing closer) the screen, we can get the changing of fringe period in both cases.

3.4. Fourier optics experiments

The scheme for Fourier optics experiments is shown in fig. 2. It is convenient to use a crossed diffraction grating (7-3) as a diffraction element.

The screen surface (20) is placed in the plane where the element (7-3) image is located. Since the element is a phase object, its image on the screen (20) will be low-contrasted.

Fourier spectrum (spatial frequency spectrum) of the object (7-3) which is similar to Fraunhofer diffraction is formed in the Fourier plane (FP). The Fourier plane location can be readily defined by a bright point given by the beam caustic (this point corresponds to the zero spatial frequency in Fourier optics). If divergence of the beam formed by collimator (6) changes, the Fourier plane (FP) will be also relocated. This scheme permits to show an invariance of Fourier image to cross shift of object similar to the Fraunhofer diffraction demonstration.

It it possible to change the image of diffraction element (7-3) on the screen (20) by overlapping of a part of the space frequency spectrum. For instance, if the zero space frequency is filtered by spatial filter (wire or small screen) we will obtain a bright image of the phase object (7-3) on a dark background ("dark field" method). A slit spatial filter located in the Fourier plane horizontally or vertically allows to filtrate vertical or horizontal space spectral components, respectively ("light field" method). A horizontal ruling of the object are visualized on a light background in the first case and vertical ones in the second case. The methods of a phase heterogeneity visualization described above belong to shadow methods and they are widely used in hydrogasdinamics, microscopy, optical monitoring, etc.

Besides demonstration of particular methods of phase contrast, the experiments considered allow imaging visually how we can realize an optical processing and identification of images by influence on some parts of a space spectrum.

It is advisible to demonstrate the Ronchi method for comparison. This method is a shadow method of defocusing diaphragm and it doesn't concern Fourier optics. But this method concurs with the phase contrast method in its function and can be realized with the scheme shown in fig. 2. An usual glass having a lot of thickness heterogeneities can be used as an object. Visualization of these heterogeneities takes place on the screen (20) if the Ronchi grating is placed close to focal plane of the lens (8).

3.5. Interferogram and reflective hologram recording

Microlens (5) is placed into laser beam to expand it (Fig. 1). A photographic plate is placed instead of turning mirror (4) to record a Denisyuk hologram.

Inclusion of recording and reconstruction of holograms into laboratory works in optics has two reasons. First, the holographic methods are widely used in science and engineering. Second, it reguires a complex applying of interference, diffraction, coherency and others notions of optics. We will illustrate the last statement by brief consideration of a physical principles of a Denisyuk hologram recording. This scheme was selected because it is more interesting from physical point of view and it is simple to realize. It should be noted that the training equipment described here allows to record a Denisyuk hologram without an additional protection against vibrations.

Fig. 5 presents an image of interference surfaces (c) resulted from the interaction between the radiation immediatly illuminating a photographic plate and the radiation passed through the plate and reflected by the object (d). It is obvious that a transparent photoemulsion should be used. If the emulsion (b) is thick enough, a number of a partially reflecting surfaces will be registered inside of the emulsion after its exposure and developing. A distance Δ between these surfaces can be estimated as $\Delta \approx \lambda / 2$ (where λ is a radiation wavelength). At a reconstruction stage, when the

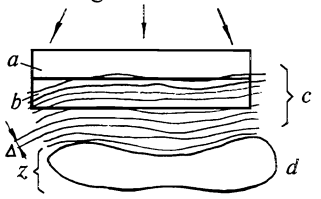

Fig. 5. Scheme for Denisyuk hologram recording. a - base; b - emulsion; c - interference surfaces; d - object; z - depth of recording scene.

hologram is illuminated by the divergent beam, the radiation reflected from each of these surfaces is characterized by a wave front which is exactly the same as the corresponding one propagated from object at the recording stage. A presence of the surfaces system allows to reconstruct hologram in a white light.
A registered scene depth (z) depends on a laser coherence length and a laser power. Z is about 50 mm for the considering set.

At the reconstruction stage we can obtain an orthoscopic virtual or pseudoscopic real image in accordance with the direction of the hologram illumination. A slide projector is a more convenient source for reconstruction of such a hologram.

Holographic interferometry possibilities can be demonstrated by recording a double-exposed hologram using the same scheme. A plane mirror is convenient to be used as an object. Before the first exposure some load (for instance 10-20 g weight) is placed in the middle of the photographic plate. This load is removed before the second exposure. On illuminating the hologram by white light two coherent monochromatic waves corresponding to the loaded and unloaded states of photographic plate are reconstructed from the hologram. The system of equal deformation isolines results from the interference of these waves. The isoline shape is determined by the load location and its curvature depends on the load mass. We can make a map of photographic plate deformations, knowing that the lightest fringe corresponds to the absence of deformation (places of plate fastening) and each next light fringe corresponds to the deformation incrementation of $\lambda / 2$.

4. GEOMETRIC OPTICS EXPERIMENTS

4.1. Experiments with Hartle device.

A modified Hartle device (incoming in the training equipment) consists of the disk (45.1) which can be turned around its axis, the stationary ring (45.2) with markes made in 10 degree intervals (45.5) and holes intended for angle of rotation fixers, the semicylindric prism (45.3) and the pointer limiting an angle of rotation.

The fixer put into hole (45.5) doesn't allow the pointer (45.6) which is rigidly mounted to the disk (45.1), to be turned more than it is set. So the incident beam may be set at reguired angle in the darkness.

For demonstration of the beam path the Hartle device (45) (fig. 1, a) is placed on the bench (23) by means of the holder (44). The bench is mounted vertically using the adapter (42). During measurements the Hartle device is fixed on the horizontal bench (23) (fig. 1).

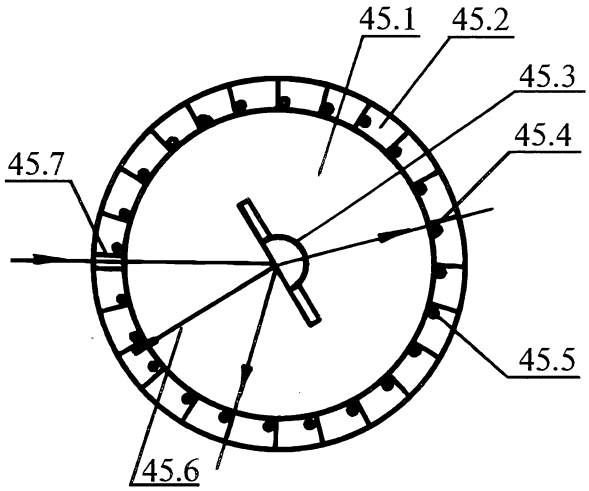

Fig. 6. Hartle device
45.1-disk; 45.2- motionless ring; 45.3-semicylindric prism; 45.4- marks; 45.5- holes for a fixers of an angle of turning ;45.6-pointer limiting an angle of turning; 45.7- cut in the ring 45.2.

4.1.1. Before demonstration of a reflected and refracted on the air-glass boundary beam path, it is necessary to make a grazing passage of laser beam above the disk (45.1). For this purpose there is the cut (45.7) in the ring frame (45.2).

The disk surface is mat which permits to observe a beam propagation in a shadowed room. The presence of marks (45.4) and the pointer (45.6) normal to planar prism surface (45.3) provides an angle of incidence, reflection and refraction to be determined with an accuracy up to 1-2 degree. Turning the disk (45.1) around its axis, we can demonstrate the corresponding beam paths and study reflection and refraction laws (Snellius-Dekart laws).

4.1.2. The laser beam enters into the prism through its cylindric surface to demonstrate the total internal reflection phenomenon. Note, that the axis of the prism cylindric surface (45.3) coincides with the axis of the disk

(45.1) rotation and the cuts (45.7) are on the disk (45.1) diameter. Therefore any beam in the Hartle device (incident, reflected or refracted one) is normal to the cylindric surface and hence, it doesn't change its direction on the boundary of air and cylindric glass surface. Selecting angle of beam incidence to the planar glass-air boundary (turning the disk (45.1)) we make the refracted beam disappear. Measuring the angle of incidence α, it is easy to determine the refraction index n of glass K-8 of which the prism (45.3) is made of according to the formula $n = 1 / \sin\alpha$.

(Refraction index of an air is taken to be 1)

4.1.3. For Brewster effect demonstration the laser beam is directed to the planar air-glass boundary and the polarizer (18) (fig. 1) is placed on the table (48). Turning the disk (45.1) and determining the direction of the reflected and refracted beam polarization in turn, we can obtain the Brewster angle whereby these beams have an orthogonal polarization.

4.1.4. Fixing the polarizer (18) by the holder (38) on the bench (23) (fig. 1) in front of the Hartle device (the radiation becomes plane polarized) and placing a photodiode on the stationary ring (45.2), we study Fresnel formulae. For such measurements the Hartle device should be fixed in the holder (44) so that the laser beam doesn't touch the disk (45.1) surface.

The photodiode holder allows change its position on the ring (45.2). The photodiode signal is recorded by the microampermeter.

4.2. Experiments using a plane-parallel cell

A plane-parallel cell is placed on the inserting support (47) which can be fixed on the optical bench (23) with the holder (44) or inserted into the table (48) (fig. 1).

4.2.1. A curvilinear light propagation.

The experiments considered are well-known, so we will present the techniques only.

A double-layer liquid is created in the cell (52): the first layer (W) is water with fluor, the second layer (S) is coloured salt solution. To do this, at first we pour some water into the cell (up to the middle) then we add a saturated (350 g/l) salt solution through a pipe submerged to the cell bottom. At the beginning the boundary will be clearly seen and it will be possible to demonstrate the total internal reflection phenomenon (fig. 7a). After a time a transition layer (W-S) with a vertical gradient of the refractive index dn / dy is forming because of diffusion. It is the reason of laser beam curving in the transition layer (W-S). Determination of the radius R of curvature of the beam path makes possible an estimation of refractive index gradient:

$$dn / dy = R.$$

When calculating of the formula we took into account that R is much larger than the beam width. This condition is fulfiled automatically since we use a nonexpanded laser beam.

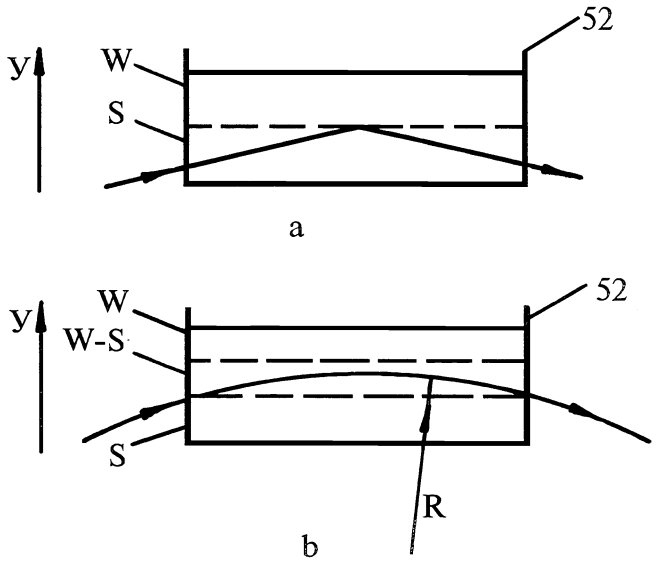

Fig. 7 Experiment with a light beam curvature. 52-planeparallel cell; W- water; S-salt solution; W-S - transition layer.

4.2.2. Optical heterogeneities visualization (shadow methods)

The scheme for optical heterogeneities visualiation is presented in fig. 8.

This scheme can be simplified by removing the lens (8-1). In this case we obtain a shadow from the cell on the screen. We will consider the case when the cell (52), lens (8-1) and screen (20) are arranged in such a way as to observe the cell image on the screen.

All effects described below are explained as a result of beams bending during their propagation through optical heterogeneity with the refractive index differing from the ambient one.

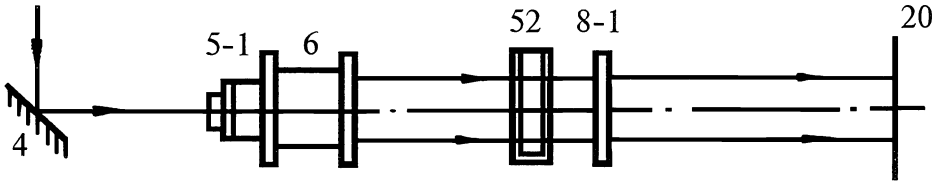

Fig. 8.
4 -turning mirror; 6 - collimator with microlens (5-1); 8-1 - lens; 20 - screen; 52 - cell.

The elements (6), (52), (8-1) are placed on the optical bench (23) (fig. 1) (the cell (52) is placed on the bench by the holder (44) and the inserting support (47)). The cell (52) is filled by water and its wide side is oriented perpendicular to the laser beam expanded by the collimator (6).

An optical heterogeneity inside the cell is created by dropping a crystal of soluble substance (for example, salt). A dynamic shadow pattern is observed on the screen (20) during the process of the crystal solution.

The experiment with an empty test-tube immersed into the cell is well known. The cell (52) (incoming in the training set) has 10 mm thickness. So we recommend to use a suitable glass tube with a stopper instead of the test-tube. We immerse the tube into the cell (52) and observe a dark tube image on the screen (20) (fig. 8).When filling the tube by water, its image on the screen (20) disappear. The demonstration will be very exciting if any opaque object is inside the tube. While tube is filled by water, the dark tube image disappears and the object image is observed.

An irregularly heated organic glass piece, a windowglass with knots and bubbles, the cell (52) with air bubbles coming to surface can also be used as objects possessing optical heterogeneity.

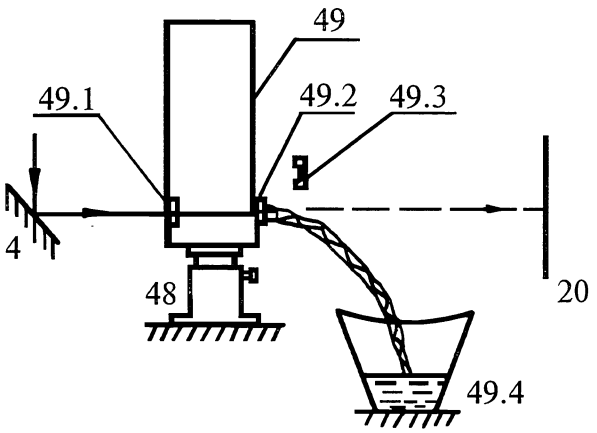

Fig. 9. Lighting jet demonstration.
4 - turning mirror; 49 - cylindric cell; 48 - in-out table; 20 - screen; 49.1 - window; 49.2 - nozzle; 49.3 - nozzle lid; 49.4 - vessel.

4.3. Lighting jet

This demonstration is useful for studying the total internal reflection phenomenon and to model a light propagation through light-guiding fiber.

The cylindric cell (49) is situated on the table (48) (fig.1) in such a way that a nonexpanded laser beam passes through the cell glass window (49.1) and the nozzle after reflection from the mirror (4). We observe a brightspot on the screen (20) or on the wall. The cell is filled by water after adjustment.

Water jet is pouring out trough the nozzle (49.2) after the lid removing. The angle of beam incedence on the jet boundary is less than the total internal reflection angle. It results in light propagation inside the jet as in light-guiding

fiber. Theoretically the light has to be observed in the place where the jet is splashing in the accepting vessel only. But the presence of air bubbles and microparticles in the jet results in a luminescence of the whole jet and the brightest luminescence is observed in the accepting vessel at the point of jet splashing.

Any glass vessel with a required volume can be used as an accepting vessel.

4.4. Demonstration of aberrations

The training equipment permits illustrating aberrations by observing the image of the lens (8-1) focal spot magnified by the microlens (5) on the screen (20).

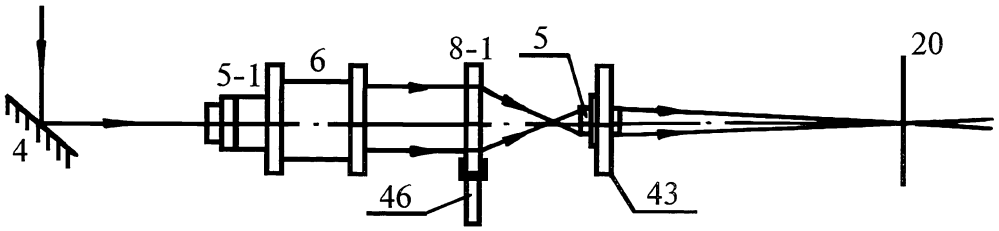

Fig. 10. The scheme for aberration demonstration .
4 - turning mirror; 6 - collimator with microlens (5-1); 8-1 - lens; 46 - turning holder; 43- microlens frame; 20- screen; 5- microlens.

It is obvious that the microlens (5) and the lens (8-1) should be co-focused which is achieved by the microlens adjustment. The lens (8-1) is fixed in the turning holder (46) and can be inclined with respect to the incoming laser beam. Furthemore, the lens (8-1) can be rolled in the holder (46) for adjustment and realizing an off-axis beam incidence.

The turning holder (46) is placed on the bench (23) (fig. 1) by the carrier (44). The microlens (5) with an additional frame (43) can be placed both in the holder (44) and on the table (48) by means of the holder (38).

The following demonstration order is preferable.

The lens (8-1) is radiated by a non-expanded laser beam (without collimator (6)) passing perpendicular to its principal planes through the lens centre. An image of an aberration-free focal spot is observed on the screen (20) (Airy spot).

When the lens (8-1) is illuminated by the expanded laser beam, a blurred circle is observed on the screen. This is a way to illustrate a spherical aberration phenomenon.

Rotating the turning holder (46) we realize tilted incidence of the expanded beam on the lens (8-1). In this case coma aberration takes place.

For astigmatism observation we use an off-axis incidence of the nonexpanded beam which is parallel to optical axis of the lens. In this case a focal spot image on the screen (20) has linear, ellipciar or circlar form, depending on the microlens position.

For demonstration of a distortion aberration it is necessary to obtain an image of square diafragm or grid created by the lens (8-1) which is placed normally to the expanded laser beam (microlens (5) in the frame (43) should be removed).

5. CONCLUSION

In this paper we present a description of a compact set of training equipment (600 by 290 by 500 mm size and less than10 kg weight) designed for use in the training purposes in optics. The basic principles of its design are the use of a laser as a light source; use of some modified optical schemes to demonstrate some classical experiments; modular structure of the set that enables one to easily modify its basic frame structure with additional modules. This approach

to the design of such a set provides a possibility of its rearrangements, when necessary, to satisfy the needs of teaching process either in high or secondary schools.

This set uses a small cw He-Ne laser delivering about 2 mW power. It provides for some demonstrations in small lecture-halls and for making certain laboratory works individually. At the same time this set can successfully be used for demonstrations with a more powerful and bigger laser, for example for demonstrations on to a large screen. Experiments with two spectral components delivered from the laser are also possible for demonstrations.

Methodological instructions provided with this set give recommendations for more than 40 demonstrations and practical works in light diffraction, interference of light, holography, geometric optics, Fourier optics, polarization effects, as well as the combination of the effects.

Among such demonstrations there are a Lloyd mirror, Newton rings, spatial filtration and shadow methods, aberrations in optical systems and so on.

Laboratory works in optics include measurement of a diffraction grating constant, curvature radii of optical surfaces, recording and reconstruction of Denisyuk holograms and so on. Demonstrations of Snellius and Malus laws, as well as Fresnel formulae are also possible.